

3D Bioprinting and Nanotechnology for Bone Tissue Engineering



Robert Choe, Erfan Jabari, Bhushan Mahadik, and John Fisher

1 Introduction

On the nanoscale, bone tissue is a composite of organic and inorganic constituents (Fig. 1) [1]. The organic phase, which makes up 30% of bone, consists of a variety of structural proteins and polysaccharides. Its main constituents are collagen fibrils that have diameters between 35 and 60 nm and can be up to 1 μm in length [2]. The remaining 10% of the organic phase consists of noncollagenous proteins that include osteocalcin, osteonectin, bone sialoprotein, bone phosphoproteins, and small proteoglycans. Additionally, these fibrils are organized with a periodicity of 67 and 40 nm gaps and are mineralized with hydroxyapatite crystals. Making up the remaining 70% of bone, the inorganic phase functions as an ion reservoir for Ca, P, Na, and Mg and provides stiffness and strength of bone in the form of apatite, carbonate, acid phosphate, and brushite. As the main component of the inorganic phase, hydroxyapatite is an anisotropic and extremely stiff inorganic component that lies in the collagen gaps [3]. This unique combination between the two phases has allowed the bone to achieve an ideal mechanical strength and architecture to support de novo bone formation.

Most bone tissue engineering (BTE) research to date has focused on mimicking the mechanical properties of the native tissue and induction of new tissue ingrowth [4]. Numerous biomaterials have been utilized to match the stiffness of bone and support bone formation. However, most have failed to integrate completely with the host tissue due to several factors that have limited bone restoration capabilities [5]. While attempts have been made to mimic the macro and microstructure of bone using porous scaffolds, these fabrication methods have not been able to fully recapitulate the complex cortical and trabecular architecture of native bone. As a result, nanostructured scaffolds based on nanomaterials have been explored to better mimic

R. Choe · E. Jabari · B. Mahadik · J. Fisher (✉)

Fischell Department of Bioengineering, University of Maryland, College Park, MD, USA

e-mail: bhushanpmahadik@gmail.com; jpfisher@umd.edu

© Springer Nature Switzerland AG 2022

F. P. S. Guastaldi, B. Mahadik (eds.), *Bone Tissue Engineering*,
https://doi.org/10.1007/978-3-030-92014-2_9

193

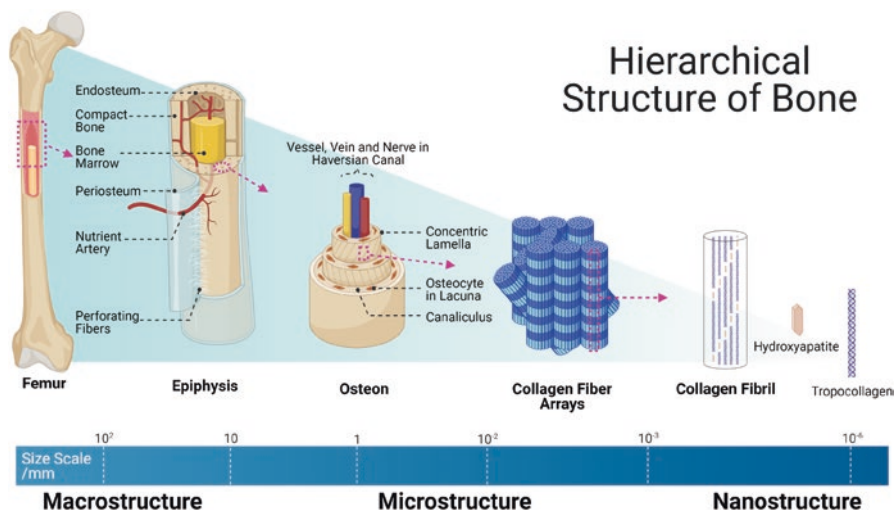


Fig. 1 Bone tissue is a complex structure consisting of organic and inorganic phases down to the nanoscale. Making up 30% of bone, the organic phase consists of a variety of structural proteins and polysaccharides. The collagen fibrils are the main constituents of the organic phase with ranging between 35 and 60 nm in diameter and up to 1 μm in length. The inorganic phase makes up the remaining 70% of bone and functions as an ion reservoir for Ca, P, Na, and Mg. Additionally, this phase provides stiffness and strength mainly in the form of hydroxyapatite. (Created with [Biorender.com](https://www.biorender.com))

the natural bone extracellular matrix (ECM) [6]. The nanotechnology utilized in these constructs has demonstrated added benefits in stimulating functional tissue due to improved cellular- and protein-level interactions [7] and has provided new avenues to engineer scaffolds with better bioactivity, cytotoxicity, and mechanical properties suitable for bone regeneration.

The purpose of this chapter is to highlight the current developments in BTE with regard to 3D bioprinting and nanotechnology. We will first introduce how 3D bioprinting has been applied in BTE and then examine various nanomaterials that have been utilized for bone regeneration. The combined application of 3D bioprinting and nanotechnology will be discussed in each section.

2 Overview of 3D Bioprinting in Bone Tissue Engineering

Additive manufacturing methods have become a more attractive approach for BTE due to their ability to replicate complex macroscale geometries using patient defect-specific scanning techniques [8]. Another advantage of these techniques is their ability to produce constructs with consistent microscale geometry, which eliminates sample to sample variability that has critical implications for future clinical translation. Additive manufacturing techniques have been available since the 1980s and

have been increasingly utilized in the tissue engineering field to fabricate bone constructs [9].

The three main 3D bioprinting strategies that have been utilized in BTE are stereolithography (SLA), extrusion printing, and inkjet printing [10]. Stereolithography, which utilizes ultraviolet (UV) light beam focused on a bed of liquid photopolymer to print layer-by-layer, is a prevalent 3D printing strategy utilized to create anatomical models to preplan orthopedic and craniofacial surgeries. While many others have utilized this strategy to manufacture biodegradable scaffolds for several decades, numerous challenges associated with SLA printing still remain, such as overcoming the toxic effects of the residual photoinitiators and the negative impact of UV light on cells [11]. In contrast, extrusion printing utilizes pneumatic or mechanical force to extrude the bioink. Due to the ability to print high viscosity bioinks and print high cell densities, extrusion-based printing still remains an attractive printing strategy for BTE [4]. However, distortion of the cell structure post-printing and low resolution of the final printed constructs remain key challenges in building upon extrusion-based printing [12]. The last printing strategy available for BTE involves inkjet printing, which utilizes thermal, piezoelectric, or electromagnetic means to deposit droplets of bioink. While this methodology provides great advantages of high speed, availability, and relatively low cost, there are major challenges involving the lack of precise droplet size and placement and its requirement for low viscosity bioinks with less than ideal mechanical properties for BTE [13]. Earlier studies involving inkjet printers used this strategy as a means to achieve indirect fabrication of the bone scaffold [14]. Nonetheless, more research needs to be done to optimize the printing parameters of inkjet printing for BTE.

All three bioprinting techniques have demonstrated promise in manufacturing BTE scaffolds. Each printing strategy offers advantages and disadvantages in terms of accessibility, cost, and resolution. Therefore, the selection of a particular bioprinting option mostly depends on the specific needs of the user. Chapter “Additive Manufacturing Technologies for Bone Tissue Engineering” provides additional details on various additive manufacturing technologies.

3 Nanomaterials in Bone Tissue Engineering

Extensive research in BTE has revealed that there are numerous physical and biological requirements in designing an ideal bone implant. Since the native bone ECM possess structures that extend down to the nanoscale, nanomaterials have been investigated to help replicate these nanostructures within the bone microenvironment and better control cell behavior. Nanomaterials possess at least one dimension that is less than 100 nm, and they have numerous advantageous traits that their micro-sized counterparts do not possess. These properties range from specific surface characteristics to superior mechanical, electrical, optical, and/or magnetic properties that are oftentimes absent in micro-sized counterparts [5]. When nanomaterials are incorporated into scaffolds, the surfaces obtain nanoscale roughness

and specific surface chemistries, wettability, and surface energies that can mimic the bone ECM [5]. Nanomaterials have demonstrated better osteoblast cell adhesion and proliferation than standard materials [7]. While the underlying mechanisms of cell response on the nanostructures are still being investigated, the unique surface topography provided by these materials plays a large role in modulating bone healing [15]. More specifically, the nanotopography introduced by the nanomaterials have been shown to affect cell adhesion, proliferation, and differentiation behavior and matrix organization [16]. Mechanistically, cell fate is influenced by changes to the surface texture, geometry, spatial position, and height of the scaffold, because these changes all affect the clustering of integrins responsible for signal transduction, development of focal adhesions, and cytoskeletal structure [17]. Additionally, nanostructures further promote protein adsorption to aid the process of cell adhesion on biomaterials [18]. These proteins ultimately help regulate cell attachment and initiate signal transduction within cells to further influence cell migration, proliferation, differentiation, and ultimately tissue formation [19].

In general, nanomaterials are subdivided into nanoparticles, nanofibers, and nanocomposites. Nanoparticles, which are particles with a size less than 100 nm in all three dimensions, have been explored to improve bone healing and provide cellular cues for osteogenesis. Nanoparticles have demonstrated the ability to enhance bone regeneration, prevent infection, and improve the outcome of implant osseointegration [20, 21]. These particles have been commonly utilized as delivery agents for bioactive molecules, cell labeling agents to monitor and target sites of interest, and supplements to improve the overall performance of bone scaffolds [5]. Nanofibers, where only two dimensions are less than 100 nm, are fibers that mimic

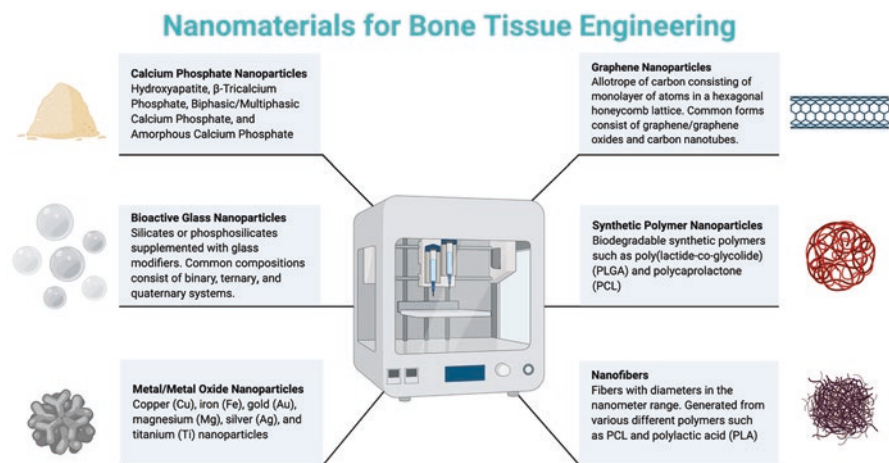


Fig. 2 Various nanomaterials have been utilized for BTE to date, which include calcium phosphates, bioactive glass, metal nanoparticles, graphene, nanofibers, and synthetic polymer nanoparticles. Recent scaffold strategies involving these nanomaterials have tried to enhance a biomaterial response to meet the mechanical and physiological demands of the host bone tissue. (Created with [Biorender.com](https://biorender.com))

the nanofibrous nature of the native ECM and provide the topographical layout to aid cell attachment [18]. Lastly, nanocomposites are composite scaffolds that utilize various combinations of nanomaterials, since bone engineering strategies utilizing only one material have not been able to fulfill the requirements of an ideal bone scaffold. Figure 2 overviews nanomaterials that have been used in BTE to date. More recent strategies have attempted to tailor a biomaterial response that can meet the mechanical and physiological demands of the host tissue capitalizing on the beneficial properties of multiple materials. The properties of specific nanomaterials in BTE and how each are incorporated into bone bioprinting will be discussed in the following subsections.

3.1 Calcium Phosphate Nanoparticles

Calcium phosphates have been extensively utilized in BTE. Table 1 summarizes current bone bioprinting studies utilizing calcium phosphate nanoparticles to date. Being composed of calcium and phosphorus ions, these minerals have demonstrated the ability to regulate the bone remodeling process by influencing osteoblast and osteoclast differentiation [48, 49]. Additionally, controlling the surface properties and porosity of calcium phosphates have also been shown to influence protein absorption, cell adhesion, and bone mineralization [50]. Depending on the type of calcium phosphate, the bioactivity will vary due to different rates of ion release, solubility, stability, and mechanical strength [51]. As the osteoconductivity and osteoinductivity of calcium phosphates are influenced by physical and chemical properties, numerous types of the mineral have been investigated for BTE applications.

Hydroxyapatite ($\text{Ca}_{10}(\text{PO}_4)_6\text{OH}_2$ or HAp) is a very common form of calcium phosphate used in BTE applications. HAp crystals make up the inorganic phase of bone, which forms needle-like 20–60 nm crystals and can be harvested from bone [52]. Various studies have established that HAp is the most stable calcium phosphate with low solubility in physiological conditions [53]. Additionally, HAp has demonstrated good biocompatibility since it does not induce an inflammatory reaction when utilized clinically [54]. The surface of HAp particles can serve as nucleating site for bone minerals in body fluids [55]. While HAp is inherently osteoconductive, additional ions such as fluoride, chloride, and carbonate ions have been incorporated to make these minerals more osteoinductive [56, 57]. Numerous studies have demonstrated the potential for HAp to improve *in vivo* bone regeneration through increased mesenchymal stem cell proliferation, due to better osteoblast adhesion, and enhanced differentiation [58].

More recent studies have demonstrated that nanohydroxyapatite (nHAp) enhances the performance of engineered scaffolds with respect to its microscale counterpart. Since the morphology of nHAp inherently leads to a greater surface area compared to micro-HAp, these nanoparticles can be densely packed as the scaffolds are fabricated [59], which significantly improves the mechanical

Table 1 Bone bioprinting with calcium phosphate nanoparticles

Study type	Calcium phosphate type	Additional constituents	Printing method	Observations	References
In vitro	Amorphous calcium phosphate	rhBMP-2	Extrusion (cryogenic 3D printing)	<ul style="list-style-type: none"> – Improved cell viability – Increased attachment, proliferation, and differentiation 	Wang et al. [22]
In vitro	β -TCP	Silver nanoparticles (AgNP)	Extrusion	<ul style="list-style-type: none"> – Constructs displayed well-defined morphology and mechanical properties suitable for bone implants – Incorporating AgNPs helped improve mechanical properties, biocompatibility, and bactericidal activity 	Correia et al. [23]
In vitro In vivo (rabbit)	β -TCP		Robocasting	<ul style="list-style-type: none"> – No immunogenicity – Increased bone formation 	Tovar et al. [24]
In vitro In vivo (rat)	β -TCP	<ul style="list-style-type: none"> – 2D black phosphorus (BP) nanosheets – P24 peptide – Doxorubicin (DOX) 	Extrusion (cryogenic 3D printing)	<ul style="list-style-type: none"> – Nanocomposites hierarchically porous and mechanically strong – Observed prompt tumor ablation and long-term suppression of tumor recurrence – BP nanosheets could control the long-term toxicity of released DOX 	Wang et al. [25]
In vitro	β -TCP	Silver nanoparticle-graphene oxide nanocomposite (Ag@GO)	Extrusion	<ul style="list-style-type: none"> – Presented excellent antibacterial activity – Accelerated osteogenic differentiation and increased osteogenic gene expression 	Zhang et al. [26]
In vitro In vivo (rabbit)	Biphasic calcium phosphate (BCP)	Platelet-rich fibrin (PRF)	Extrusion	<ul style="list-style-type: none"> – Sustained release of bioactive factors – Improve biocompatibility and bioactivity – Induced greater bone formation than BCP/PVA scaffolds 	Song et al. [27]

Study type	Calcium phosphate type	Additional constituents	Printing method	Observations	References
In vitro	Citrate-HAp	Minocycline	Fused deposition modeling	<ul style="list-style-type: none"> - Uniform macroporosity, adequate wettability and excellent compressive strength - Citrate-HA stimulated adhesion, proliferation and differentiation - Antimicrobial 	Martin et al. [28]
In vitro	Mineral-substituted HAp (Mg-HAp)		Extrusion	<ul style="list-style-type: none"> - Scaffolds smoother than HAp scaffolds - More acidic conditions due to Mg ion release - Higher cell attachment, proliferation, and increased osteogenic gene expression 	Chen et al. [29]
In vitro In vivo (rabbit)	Mineral-substituted HAp (Sr-HAp)		Extrusion	<ul style="list-style-type: none"> - Enhanced cell adhesion, proliferation and ALP activity 	Luo et al. [30]
In vitro	nHAp	Compatibilized MgF ₂ (cMgF ₂) nanoparticle	Extrusion	<ul style="list-style-type: none"> - Stimulated more bone formation - Enhanced mechanical and biological properties - Improved osteogenic differentiation and stimulated mineralization 	Bas et al. [31]
In vitro	nHAp	Core-shell PLGA/TGF-β1 nanospheres	SLA	<ul style="list-style-type: none"> - Fabricated highly interconnected osteochondral scaffold with hierarchical structure and spatiotemporal bioactive factor gradients - Improved hMSC adhesion, proliferation, and directed osteochondral differentiation 	Castro et al. [32]

(continued)

Table 1 (continued)

Study type	Calcium phosphate type	Additional constituents	Printing method	Observations	References
In vitro	nHAp	Chitosan/sodium hyaluronate (CS/SH) coating	Extrusion	<ul style="list-style-type: none"> - Decreased swelling ratio - Increased compressive strength - Slow degradation - Successful loading and release of growth factors 	Chen et al. [33]
In vitro In vivo (rabbit)	nHAp	<ul style="list-style-type: none"> - Vancomycin - Levofloxacin 	Fused deposition modeling	<ul style="list-style-type: none"> - Ability to load and release vancomycin and levofloxacin for antibacterial effect - Demonstrate osteogenic and osteoconductive potential 	Chen et al. [34]
In vitro	nHAp		Extrusion	<ul style="list-style-type: none"> - Higher elastic moduli - Improved mechanical properties - More bioactive 	Demirtas et al. [35]
In vitro In vivo (rabbit)	nHAp	rhBMP-2/chitosan nano-sustained release carrier	Extrusion	<ul style="list-style-type: none"> - Exhibited early burst and controlled release of rhBMP-2 - Biocompatible and induced osteogenic effect - Successful bone repair in rabbit mandible 	Deng et al. [36]
In vitro	nHAp	Bioactive glass	Thermal inkjet printing	<ul style="list-style-type: none"> - HAp scaffolds more effective for cell viability, increased compressive modulus, and hMSC osteogenesis than bioactive glass scaffolds 	Gao et al. [37]
In vitro	nHAp	Carbon nanotubes (CNT)	Extrusion	<ul style="list-style-type: none"> - CNT scaffold with 2 wt% offers the best combination of mechanical properties and electrical conductivity - Scaffold demonstrated typical HAp bioactivity and cell adhesion/proliferation behavior 	Goncalves et al. [38]

Study type	Calcium phosphate type	Additional constituents	Printing method	Observations	References
In vitro	nHAp		Extrusion	<ul style="list-style-type: none"> - Adequate mechanic strength and elastic behavior - Flow properties similar to native blood vessels - Enhanced hMSC adhesion, proliferation, and differentiation 	Holmes et al. [39]
In vitro	nHAp		Extrusion with thermally induced phase separation (TIPS)	<ul style="list-style-type: none"> - Fabricated a large-dimension nanofibrous scaffold with defined architecture - Enhanced fibronectin absorption, hMSC adhesion, and osteogenic differentiation 	Prasophum et al. [40]
In vitro In vivo (rabbit)	nHAp		Extrusion	<ul style="list-style-type: none"> - Observed uniform sonocoated nHAp layer of 200–300 nm - Stimulation of new bone tissue formation 	Rogowska-Tyiman et al. [41]
In vitro	nHAp	<ul style="list-style-type: none"> - MgO nanoparticle - O₂ and N₂ plasma treatment 	Extrusion	<ul style="list-style-type: none"> - Enhanced adhesion, proliferation, and differentiation of preosteoblast cells - Plasma treatment also affected behavior of cells due to changes in surface morphology/chemistry 	Roh et al. [42]
In vitro	nHAp		Extrusion	<ul style="list-style-type: none"> - Fabricated scaffolds with well-defined layers with interconnected pores - Scaffolds exhibited a controlled HAp gradient 	Trachtenberg et al. [43]

(continued)

Table 1 (continued)

Study type	Calcium phosphate type	Additional constituents	Printing method	Observations	References
In vitro In vivo (rat)	nHAp	Atstrin	Extrusion	<ul style="list-style-type: none"> – Scaffold exhibits precise structure – Sustained release of atstrin – Minimal cytotoxicity and supports cell adhesion – Enhanced bone regeneration 	Wang et al. [44]
In vitro	nHAp (modified with dopamine and hexamethylenediamine)		Extrusion	<ul style="list-style-type: none"> – Robust mechanical properties – Good biocompatibility – Support proliferation and osteogenic differentiation 	Yang et al. [45]
In vitro	nHAp		Extrusion	<ul style="list-style-type: none"> – Increased ALP activity and mineralization – Improved preosteoblast proliferation and differentiation 	Yu et al. [46]
In vitro	nHAp	TGF- β 1 PLGA nanoparticle	SLA	<ul style="list-style-type: none"> – Promoted osteogenic and chondrogenic differentiation – Enhanced osteogenic and chondrogenic gene expression 	Zhou et al. [47]

properties of the scaffold [60]. Additionally, the increased surface area of nHAp drastically improves protein adsorption capabilities compared to larger HAp particles [61]. Synthesized nHAp can be fabricated as rods, fibers, or particulates due to the different modes of synthesis [62, 63]. Since nHAp is very similar to native bone in terms of size and chemistry, it has firmly established itself as a favorable material for BTE.

Research has demonstrated that nanohydroxyapatite can be successfully incorporated into bone bioprinting strategies. The most prevalent approach involves adding nHAp to synthetic polymer such as polycaprolactone (PCL) [39]. While some groups resorted to coating the scaffold surface with nHAp post-printing, others have successfully mixed the nHAp particles directly into the bioink formulation for extrusion printing. Trachtenberg et al. utilized an extrusion-based printing strategy to develop poly(propylene fumarate) (PPF) scaffolds with a mineral gradient within the scaffold (Fig. 3) [43]. In order to improve the dispersion of the nHAp particles within the scaffold, a surfactant was added to the print formulation without compromising the compressive strength overall. The printed PPF composite scaffolds with nHAp nanoparticles consisted of well-defined layers with interconnected pores that could potentially serve as mechanically robust bone implants. Few groups have proceeded on to functionalize scaffolds with even more constituents to create complex

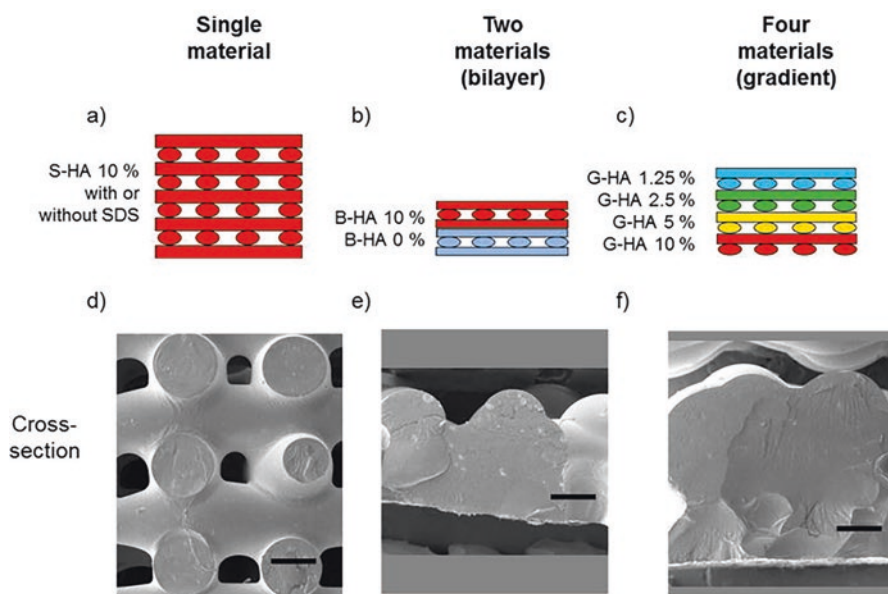


Fig. 3 Schematic of printed scaffolds. (a) PPF-HA (10 wt%) scaffold with or without SDS. (b) PPF-HA bilayer scaffold containing PPF and PPF-HA (10 wt%). (c) PPF-HA gradient scaffold containing layers of 1.25, 2.5, 5, and 10 wt% HA. Respective SEM cross-sections of (d) a PPF-HA scaffold with or without SDS, (e) a PPF-HA bilayer scaffold, and (f) a PPF-HA gradient scaffold. Pore interconnectivity is lost with the addition of multiple materials. Scale bars in (d–f) represent 0.5 mm. (Reprinted by permission of the publisher (Taylor & Francis Ltd.) [43])

multiphase scaffolds. Deng et al. recently fabricated poly(lactic-*co*-glycolic) acid (PLGA)/nHAp/chitosan (CS)/rhBMP-2 scaffolds with an extrusion printer [36]. CS nanospheres encapsulating rhBMP-2 were embedded within a CS hydrogel to prepare a nano-sustained release carrier, which was then co-printed with PLGA/nHA bioink to create the composite scaffold. The scaffold complex demonstrated an effective controlled burst release of rhBMP-2 that further aided in osteogenesis within mandibular bone defects. Others have loaded antibiotics within these composite scaffolds to introduce an antibacterial effect with good results [28].

Some groups have explored the use of hydrogel incorporated with nHAp for bone bioprinting. Wang et al. 3D printed alginate/nHAp scaffolds incorporated with atsttrin, which is a progranulin-derived engineered protein that exerts an antagonistic effect on proinflammatory TNF- α [44]. This composite scaffold was able to demonstrate sustained release of the atsttrin that enhanced the bone regeneration within a mouse calvarial defect. Another group successfully printed chitosan/nHAp scaffolds that had superior cell proliferation and differentiation capabilities compared to alginate-based scaffolds [35]. However, hydrogels are still challenging to use as a bone scaffold due to inadequate mechanical properties. In order to enhance the mechanical and bioactive properties of hydrogel scaffolds, Chen et al. extrusion printed with a bioink formulation consisting of 60% nHAp particles and 40% gelatin/hyaluronate hydrogel [33]. These scaffolds were lyophilized and then coated with multiple layers of chitosan and sodium hyaluronate, which significantly helped improve the compressive strength and ability to load growth factors onto the scaffold surface.

Tricalcium phosphate ($\text{Ca}_3(\text{PO}_4)_2$ or TCP) is another common calcium phosphate utilized in bone regeneration other than HAp [51]. While two phases of TCP exist, β -TCP is generally used in bone regeneration due to its more stable structure and higher biodegradation rate [64]. Additionally, β -TCP degrades faster and is more highly soluble than HAp, which leads to a higher resorption rate and increase biocompatibility [65]. β -TCP also promotes proliferation of osteoprogenitor cells due to its inherent nanoporous structure that enables excellent biomineralization and cell adhesion [66]. Therefore, numerous groups have utilized β -TCP as the main additive for bone bioprinting. Tovar et al. successfully robocasted 100% β -TCP scaffolds that were biocompatible, resorbable, and could anisotropically regenerate bone within a rabbit model [24]. Additionally, Wang et al. fabricated a complex β -TCP/PLGA scaffold with a novel cryogenic 3D printer involving water-in-oil polyester emulsion inks with multiple functional agents—2D black phosphorus nanosheets, doxorubicin hydrochloride, and BMP-2-like osteogenic peptide (P24) [25]. The group was able to print hierarchically porous and mechanically strong scaffolds that can be potentially applied for large defect repair.

Lastly, calcium phosphates with variable compositions have also been utilized during bone bioprinting. To capitalize on the beneficial properties of both nHAp and β -TCP, some groups have utilized biphasic calcium phosphate within bone-engineered scaffolds. Biphasic or multiphasic calcium phosphates are homogeneously mixed at the submicron level to make the separation of each constituent difficult [67]. Song et al. used low-temperature robocasting to fabricate a 3D printed

ceramic scaffold composed of nano-biphasic calcium phosphate, polyvinyl alcohol, and platelet-rich fibrin [27]. Without the addition of toxic chemicals during the printing process, the group demonstrated that these composite scaffold could be printed with the desired internal and external architecture while enhancing bone defect repair with the incorporated bioactive factors. Also possessing intermediate properties, amorphous calcium phosphate ($\text{Ca}_3(\text{PO}_4)_2 \cdot n\text{H}_2\text{O}$) is a less-ordered, transition phase calcium phosphate that serves as a precursor state that precedes biological apatite formation [68]. Since the mineral in natural bone is composed of poorly crystalline, highly substituted apatite nanocrystals interspersed within a collagen matrix, one potential bone regenerative strategy is to deposit a less ordered mineral phase to mimic the biomineralization process [55]. Wang et al. demonstrated that PLA scaffolds loaded with amorphous calcium phosphate nanoparticles with rhBMP-2 could improve cell viability, attachment, proliferation, and differentiation for BTE applications [22].

3.2 *Bioactive Glass Nanoparticles*

Bioactive glass nanoparticles (BGNP) are another class of ceramic nanoparticles that are commonly used in bone regeneration due to their high bioactivity and great bone bonding properties [69]. BGNPs are generally comprised of silicates or phosphosilicates supplemented with distinct proportions of glass modifiers like sodium oxide (Na_2O) and calcium oxide (CaO) [69]. The common compositions of BGNPs are binary (e.g., $\text{SiO}_2\text{-CaO}$), ternary (e.g., $\text{SiO}_2\text{-CaO-P}_2\text{O}_5$), or quaternary systems (e.g., $\text{SiO}_2\text{-CaO-P}_2\text{O}_5\text{-Na}_2\text{O}$), which in turn affects the porous structure and surface area of the BGNPs [70–72]. Most BGNPs possess a spherical morphology, but non-spherical BGNPs have also been generated in the form of pineal or rod shapes [73, 74]. Some reports have indicated that spherical nanoparticles may be taken up by the cell more quickly and efficiently than non-spherical nanoparticles [75]. However, non-spherical nanoparticles present a more biomimetic morphology analogous to the natural HAp structural units, which can ultimately improve the mechanical properties and biomineralization capability more ideal for bone scaffolds [76].

Decreasing the dimensions of the bioactive glass particles down to the nanoscale increases the specific surface area, pore size, and ion exchange capabilities compared to bioactive glass microparticles [77]. In effect, BGNPs are able to generate a calcium phosphate layer more quickly due to improved exposure to the bioactive elements. Ajita et al. highlighted how nanoscale bioactive glass particles could affect the proliferative behavior in mouse MSCs [78]. The group demonstrated that all BGNPs administered at 20 mg/mL showed no cytotoxic effect, but the cells treated with smallest nanoparticles (37 nm) experienced the greatest increase in cell proliferation. The faster ion release rate and the increased surface area improve protein adsorption, which in turn promote cell adhesion, proliferation, and differentiation. Some studies have indicated that calcium silicate exhibits better

Table 2 Bone bioprinting with bioactive glass nanoparticles

Study type	Calcium phosphate	Additional constituents	Printing method	Observations	References
In vitro	Bioactive glass (SiO ₂ -CaO-P ₂ O ₅ with weight ratio 80:15:5)	Poly(citrate-siloxane) (PCS)	Extrusion	<ul style="list-style-type: none"> -Scaffolds with BG-PCS presented superior elasticity and superior compressive strength -Controlled release of Si and Ca ions and enhanced biomineralization -Promoted cell attachment, proliferation, and enhanced osteogenic differentiation 	Chen et al. [80]
In vitro In vivo (mouse)	Bioactive glass (SiO ₂ -CaO-P ₂ O ₅ with weight ratio 70:25:2.5)	CuFeSe ₂ nanocrystals (CFS)	Extrusion	<ul style="list-style-type: none"> -Varying the concentration of the CF crystals and laser power density helped regulate photothermal performance of scaffold -BG-CFS scaffolds could stimulate osteogenic gene expression and new bone formation 	Dang et al. [81]
In vitro	Bioactive glass (bioglass 45S5 or SiO ₂ -CaO-Na ₂ O-P ₂ O ₅ with weight ratio 45:24.5:24.5:6)	nHAp	Thermal inkjet printing	<ul style="list-style-type: none"> -HAp scaffolds more effective for cell viability, increased compressive modulus, and hMSC osteogenesis than bioactive glass scaffolds 	Gao et al. [82]
In vitro	Bioactive glass (SiO ₂ -B ₂ O ₃ -CaO-Na ₂ O-P ₂ O ₅ -MgO-SrO with weight ratio 47.12:6.73:6.77:22.66:1.72:5:10)	Wood-based nanocellulose (CNF)	Extrusion	<ul style="list-style-type: none"> -Cells less viable and proliferative in BG bioinks -Constant increase in ALP activity observed in all hydrogels -hBMSC tolerated bioprinting process better than Saos-2 cells 	Ojansivu et al. [83]

Study type	Calcium phosphate	Additional constituents	Printing method	Observations	References
In vitro In vivo (mouse)	Bioactive glass (SiO ₂ -CaO-P ₂ O ₅ with weight ratio 80:15:5)	Mesoporous silica nanosphere (MSN) - Isoniazid - Rifampin	Extrusion	- Scaffolds demonstrated prolonged drug release - Displayed good osteogenic potential	Zhu et al. [84]
In vitro	Laponite®		Extrusion	- Improved stability at physiological conditions - No change in mechanical stiffness - Improved bioactivity, hMSC proliferation, and differentiation	Carrow et al. [85]
In vitro Ex vivo (chick chorioallantoic membrane)	Laponite®		Extrusion	- Scaffold displayed enhanced shape retention and interconnected porosity - Improves hBMSC viability, attachment, proliferation, and differentiation - Scaffold supports cell growth and retention/delivery of growth factors	Cidonio et al. [86]
In vitro Ex vivo (chick chorioallantoic membrane)	Laponite®		Extrusion	- Significant potential in printing fidelity, tailorable swelling characteristics, and enhanced shape retention - Laponite increased cell-laden bioink functionality - Absorption/release properties depended on Laponite incorporation	Cidonio et al. [87]
In vitro Ex vivo (chick chorioallantoic membrane) In vivo (mouse)	Laponite®	- BMP-2 - VEGF	Extrusion	- Demonstrated elevated viability and functionality in vitro, ex vivo, and in vivo	Cidonio et al. [88]

(continued)

Table 2 (continued)

Study type	Calcium phosphate	Additional constituents	Printing method	Observations	References
In vitro In vivo (rat)	Laponite®		Extrusion	<ul style="list-style-type: none"> – Demonstrated improved proliferation and differentiation than PEG-clay scaffolds – Scaffold possesses excellent osteogenic potential 	Zhai et al. [89]
In vitro	Polydopamine-modified calcium silicate (CaO-SiO ₂ -Al ₂ O ₃ -ZnO with weight ratio 65:25:5:5)		Extrusion	<ul style="list-style-type: none"> – PDACS/PCL experienced more cell attachment and proliferation due to improved hydrophilicity – Scaffolds showed increased osteogenic and angiogenic potential 	Chen et al. [79]

biodegradation and osteoconductivity than calcium phosphate, which has led to research adding these powders into the 3D bioprinting process [79].

Various bioactive glass nanoparticles have been explored for bone bioprinting. Table 2 summarizes current bone bioprinting studies utilizing bioactive glass nanoparticles to date. Carrow et al. extrusion-printed bioactive nanocomposites by incorporating 2D nanosilicates into a co-polymer (PEOT/PBT) scaffold [85]. The inclusion of nanosilicates improved the stability and bioactivity of the scaffold under physiological conditions without compromising the mechanical stiffness of the printed scaffold. Laponite nanoclay, a type of nanosilicate similar to hectorite, was also utilized in several different hydrogel nanocomposites to demonstrate improved printability and mechanical stability of the printed constructs, without compromising cell viability and distribution [86–89]. Current research has demonstrated that these nanoparticles possess a versatile ability to functionalize additional components onto their surface. Luo et al. integrated the adhesion peptide (RGD sequence) onto mesoporous silica nanoparticles to dually functionalize bone forming peptide-1 [90]. This dual-peptide-loaded alginate hydrogel system promoted the sequential differentiation of hMSCs. Some groups have also succeeded in functionalizing photothermal or photoluminescent components onto these nanoparticles, opening up the possibility of utilizing them for bioimaging, tumor therapy, and bone regeneration applications [80, 81]. Lastly, few groups have begun to develop ternary nanocomposites with additional biopolymers to supplement more bioactivity, mechanical advantages, and cell attachment potential within the printed construct [83, 91].

3.3 *Metal and Metal Oxide Nanoparticles*

Metals have been widely explored as a material to replace bone tissue, primarily because of their strong mechanical properties to withstand physiological forces experienced by bone. While most research into the area has utilized metals as the major implant component, recent studies have demonstrated the potential of utilizing metal nanoparticles to enhance the bioactivity of the implants.

Titanium-Based Nanoparticles

Titanium and its alloys are some of the most explored metals to date due to their ideal mechanical properties, resistance to corrosion, and no cytotoxic effect when implanted in the body [92]. Therefore, titanium-based implants are often utilized to repair critical-sized bone defects [93]. Some studies have begun to investigate composite scaffolds that incorporate titanium nanoparticles for bone regeneration. Rasoulianboroujeni et al. recently printed a nanocomposite scaffold, comprised of PLGA and TiO₂ nanoparticles with an extrusion printer [94]. Incorporation of the nanoparticles improved the compressive modulus of the scaffolds, enhanced the

wettability of the scaffold surface, and increased osteogenic proliferation and mineralization. Another group fabricated a hybrid polymer (Ormocomp[®]) scaffold doped with barium titanite (BaTiO_3) nanoparticles via two photon lithography [95]. Preliminary in vitro testing demonstrated enhanced cell differentiation due to the refined architecture generated and the piezoelectric cues from this printing strategy.

Magnesium-Based Nanoparticles

Magnesium has been explored in bone bioprinting since it is biocompatible, regulates the density and structure of bone apatite, and mediates cell–ECM interactions [96]. Roh et al. utilized magnesium oxide (MgO) nanoparticles as a bioink additive during extrusion printing [42]. A composite scaffold comprised of PCL, HAp, and MGO contributed to enhanced adhesion, proliferation, and differentiation of cells within the scaffold. Another group developed a ternary nanocomposite consisting of PCL, nHA powder, and compatibilized magnesium fluoride nanoparticle (cMgF_2) fillers with enhanced mechanical and biological properties through extrusion printing [31]. The incorporation of cMgF_2 nanoparticles particularly led to significant improvements in the mechanical properties within the scaffolds, enhanced osteogenic differentiation, and stimulated mineralization.

Metal Nanoparticles with Antimicrobial Properties

Chronic implant-related bone infections are a major problem in orthopedic and trauma-related surgery with serious consequences that can affect the final prognosis of bone implants [97]. As a result, silver nanoparticles (AgNP) with antimicrobial properties have been incorporated into 3D printed bone scaffolds. Jia et al. demonstrated that the addition of silver nanoparticles on titanium alloy meshes helped reduce bacterial biofilm buildup, especially in combination with antibiotic therapy [98]. Silver nanoparticles have also been incorporated into extrusion printed ceramic/polymer scaffolds, further establishing their potential to enhance biocompatibility, mechanical properties, and osteogenic activity [26, 99]. Besides AgNPs, several other metal nanoparticles with antimicrobial properties have been investigated with bone bioprinting. Zou et al. recently incorporated copper-loaded-ZIF-8 nanoparticles within PLGA scaffolds through extrusion printing and found that these scaffolds possessed enhanced antibacterial and osteoconductive properties [100]. Additionally, 3D printed zirconia ceramic hip joints with a coating of ZnO nanoparticles also demonstrated antibacterial properties while maintaining the benefits of precise structure and wear resistance [101].

Iron-Based Nanoparticles

Iron oxide (Fe_2O_3) nanoparticles, being in the ferrimagnetic class of magnetic materials, have various preclinical and therapeutic uses [102]. On top of retaining the bioactivity of nanomaterials, magnetic iron nanoparticles are able to directionally aggregate and localize under a constant magnetic field. Consequently, iron oxide nanoparticles can couple to the cell surface and control cell functions such as MSC differentiation [103]. Huang et al. developed a novel diphasic magnetic nanocomposite scaffold utilizing low-temperature deposition manufacturing [104]. These scaffolds demonstrated good biocompatibility and mechanical properties, while also promoting cell differentiation. Another group incorporated presynthesized iron oxide nanoparticles into polyamide scaffolds fabricated on a selective laser sintering (SLS) printer [105]. These nanoparticles demonstrated the ability to heat up rapidly in response to an applied AC magnetic field, offering a potential avenue to remotely induce controlled gene expression within cells on these scaffolds. At the very least, iron oxide nanoparticles possess osteogenic and radiopaque properties that can be used to develop biodegradable and radiographically detectable bone implants that can aid in diagnostics and bone healing [106].

Gold-Based Nanoparticles

One nanoparticle that has not been fully utilized in bone bioprinting are gold nanoparticles (AuNPs), which have become a promising tool in nanomedicine due to their nanoscale dimensions, ease of preparation, high surface area, and functionalization capability [107]. Therefore, some groups have investigated how AuNPs can promote osteogenic differentiation in stem cells. Choi et al. demonstrated that chitosan-conjugated AuNPs increase the calcium content and osteogenic gene expression at non-toxic concentration through the Wnt/ β -catenin signaling pathway. The particle size also appears to play a role in MSC differentiation, as 30 and 40 nm AuNPs were taken up by the MSCs, the most and consequently demonstrated the highest cell differentiation rates [108]. Some groups have explored functionalizing AuNPs to influence the MSC behavior. Li et al. functionalized gold nanoparticles with various chemical groups to find that amino-functionalized AuNPs exhibited increased ALP expression and matrix mineralization [109]. AuNPs can also serve as a suitable protein or peptide delivery mechanism, as Schwab et al. were able to assess the impact of surface immobilized BMP-2 on the Smad signaling pathway with these particles [110]. The group utilized nanolithography to create a precisely spaced, tunable gold nanoparticle array embedded with single BMP-2 molecules. Compared to the control condition consisting of soluble BMP-2, the AuNP-immobilized BMP-2 demonstrated a prolonged and elevated intracellular signal transduction that could help upregulate the TGF β superfamily growth factors to further stimulate bone regeneration.

3.4 Graphene Nanomaterials

Graphene is a novel nanomaterial that has potential applications for BTE. With exceptional conductivity and physiochemical and mechanical properties, these thin carbon sheets with large surface area can significantly improve the properties of the composite at minute concentrations. Graphene has an aromatic configuration that been reported to promote cell attachment, growth, proliferation, and differentiation [111]. Choe et al. utilized an extrusion printer to fabricate alginate/graphene oxide (GO) composites to improve the printability, structural stability, and osteogenic potential of scaffolds [112]. This bioink formulation demonstrated high printability and stability and was able to maintain high cell viability and stimulate osteogenic differentiation. Another study printed polylactic acid (PLA) scaffolds incorporated with GO using fused deposition modeling (FDM) printer [113]. The addition of GO increased the surface roughness, hydrophilicity, and mechanical properties of the PLA/GO scaffolds. Additionally, the PLA/GO scaffolds proved to be more biocompatible and promoted cell proliferation and mineralization more efficiently than pure PLA scaffolds.

Some researchers have also incorporated carbon nanotubes (CNT) into bone tissue regeneration. CNTs are a variation of a single graphene sheet that is rolled up into a hollow cylindrical nanostructure and are commonly divided into either single-walled carbon nanotubes (SWCNT) or multi-walled carbon nanotubes (MWCNT) [114]. SWCNTs are formed from a single tubular graphene while MWCNTs consist of multiple concentric tubular graphene layers. Their unique nanoscale cylindrical shape makes them capable delivery agents for various biomolecules and drugs [115]. CNTs offer great strength, elasticity and fatigue resistance that can help reinforce composite scaffolds for bone regeneration [116]. With enhanced mechanical properties, CNTs are able to create a strong bond on composite scaffolds that facilitates load transfer and strengthens the scaffold matrix [117]. Additionally, CNTs are more conducive to protein adsorption and cell attachment due to their high specific surface area resulting from their highly porous structure [118, 119]. This porous interlinked nanostructure is favorable for nutrient transport throughout the bone matrix. CNTs can also influence cell morphology and promote osteogenesis with modifications to their surface chemistry and affinity for cell-binding proteins [120].

Recent studies have examined how CNTs can be incorporated into the bioprinting process. Huang et al. fabricated a porous PCL/MWCNT composite scaffold utilizing an extrusion printer (Fig. 4) [121]. The addition of the MWCNT improved protein adsorption, mechanical and biological properties of the scaffolds, indicating that these composite scaffolds can be a viable candidate for bone tissue regeneration. Another group similarly developed a three-phase nanocomposite scaffold with nHAp, CNTs, and PCL via extrusion printing [38]. They also found that the composite scaffolds demonstrated typical bioactivity, good cell adhesion, and

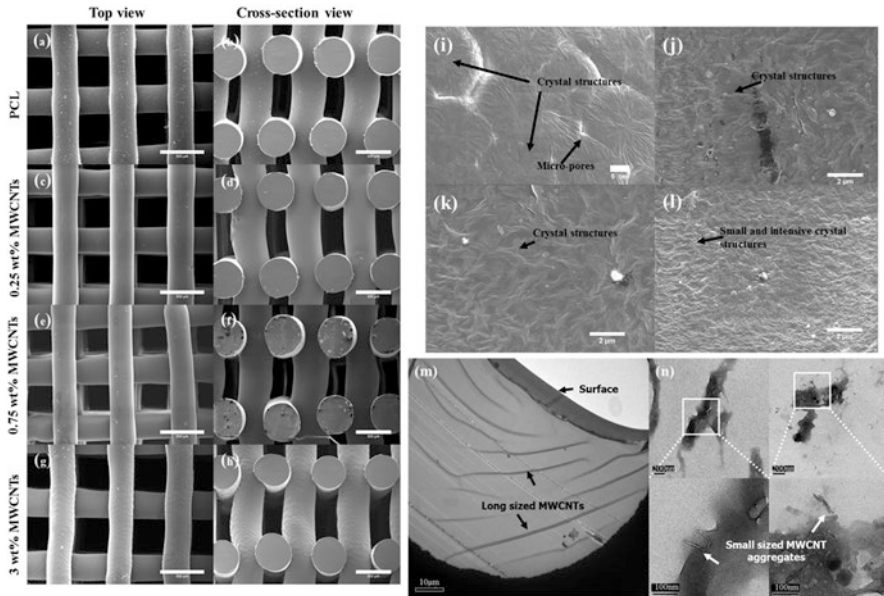


Fig. 4 SEM images of (a) top view and (b) cross-section view of PCL scaffold, (c) top view and (d) cross-section view of PCL/MWCNT 0.25 wt% scaffold, (e) top view and (f) cross-section view of PCL/MWCNT 0.75 wt% scaffold, and (g) top view and (h) cross-section view of PCL/MWCNTs 3 wt% scaffold; High-magnification SEM images showing spherulites in the PCL matrix and boundaries between crystal structures in the filament surface of (i) PCL, (j) 0.25 wt%, (k) 0.75 wt%, and (l) 3 wt% PCL/MWCNT composite scaffolds; TEM images showing (m) the alignment and migration of long-length MWCNTs, (n) the agglomeration of short-length MWCNTs in PCL/MWCNT 3 wt% [121]

proliferation with added mechanical performance and electrical conductivity from CNT. These graphene-based nanocomposites show promise as they help improve the mechanical properties and cytocompatibility within scaffolds. However, more work is being done to effectively synthesize these novel CNT-based nanocomposites. Liu et al. were able to effectively print PPF scaffolds with negatively charged CNT/ssDNA nanocomplexes through stereolithography [122]. Their rapid and homogenous functionalization process helped coat the scaffold surface to promote adhesion, proliferation, and differentiation of the cells. Another group explored incorporating carbon nanotubes within a hydrogel [123]. Utilizing a polyion complex composed of poly(sodium *p*-styrene sulfonate) and poly(3-(methacryloylamino) propyl triethylammonium), a tough hydrogel with MWCNT was formulated to manufacture 3D scaffolds via extrusion printing. These composite scaffolds demonstrated biocompatibility and facilitated osteogenic differentiation, suggesting that hydrogels with CNTs can be used to enhance the efficiency of bone repair.

3.5 *Synthetic Polymer Nanoparticles*

Biodegradable synthetic polymers have been among the most investigated polymers due to good biocompatibility, mechanical properties, and rates of degradation that are comparable to the bone turnover rate [124]. Synthetic polymer nanoparticles have garnered much interest as a drug delivery mechanism because they have controlled degradability and have shown the potential to deliver small molecules, nucleic acids, and proteins [125, 126]. These nanoparticles are superior to conventional drug delivery mechanisms because they are more readily available, can undergo controlled release over a longer duration of time, and minimize undesirable effects such as toxicity and immunogenicity [127].

Past research has demonstrated that PLGA nanoparticles can maintain a sustained release of BMP-2 to support bone healing in vivo [128]. Kim et al. investigated the performance of a 3D-printed calcium phosphate scaffold coated with a layer of PLGA nanoparticles loaded with BMP-2 [129]. The group was able to achieve a uniform distribution of the nanoparticles and a gradual release of BMP-2. Additionally, higher de novo bone formation was observed in vivo. However, there are limited studies that have directly incorporated the polymer nanoparticles into the 3D printing process. Another study fabricated novel biphasic nanocomposite scaffolds for osteochondral regeneration that incorporated nHAp and TGF- β 1-loaded PLGA nanoparticles through stereolithography [32]. These scaffolds demonstrated that a biomimetic graded construct could be printed with hydrogels and offers a strategy to develop an implant for orthopedic application.

3.6 *Nanofibers*

Nanofibers are a valuable tool in tissue engineering for their ability to simulate the physical and biochemical environment of the natural bone ECM. Several strategies have been utilized to produce nanofibers, including phase separation and self-assembly [130, 131]. The most ubiquitous fabrication method to produce nanofibers is electrospinning, which controls the extrusion of the polymer fibers through the use of an electric field [132]. Yao et al. recently fabricated 3D nanofibrous scaffolds utilizing solely electrospinning [133]. The group demonstrated that PCL/PLA nanofibrous scaffolds, with respect to neat PCL scaffolds, possessed greater mechanical properties while enhancing cell viability of hMSCs and osteogenic differentiation in vitro and in vivo. The improved performance of the copolymer nanofibrous scaffold was noted to be attributed to the higher mechanical stiffness and bioactivity introduced by PLA itself. However, since the densely packed nanofibers lead to a distinctly smaller pore space, tissue ingrowth can be negatively affected within these scaffolds [134]. Additionally, the mechanical performance of nanofibrous scaffolds are poorer in comparison to other tissue-engineered constructs due to their large surface area-to-volume ratios and high porosities [135].

An alternative strategy is to incorporate both electrospinning and extrusion printing into the scaffold fabrication process. Since extrusion printed scaffolds often suffer from low print resolution, nanofibers have been infused into the 3D printed scaffold to introduce nanoscale features within the overall construct [136]. Vasquez-Vasquez et al. were able to show that incorporating a PLA nanofiber coating on a PLA scaffold promoted bioactivity, cell attachment, and proliferation when compared to neat PLA scaffolds [137]. Even though both the scaffold and nanofibers were synthesized with the same polymer, the nanotopographical changes introduced by the nanofibers enhanced the overall performance of the tissue construct. Nanofibers can also be functionalized with various bioactive molecules through encapsulation or surface immobilization. Li et al. examined the performance of bioactive glass short nanofibers functionalized with BMP-2 on 3D-printed PCL scaffolds [135]. Immobilizing BMP-2 onto the scaffold surface through nanofibers allowed enhanced osteogenic gene expression of bone marrow MSCs, further demonstrating that expanded applications that can be incorporated into a BTE approach of combining 3D printing and electrospinning.

Few studies have directly incorporated nanofibers directly into the bioink before the printing process. Thermoplastic polymer printing has limitations due to high temperature and pressure that can interfere with the integrity of the print [138]. Therefore, hydrogels have offered a low-temperature printing strategy that bypasses some of the issues associated with synthetic polymer printing. Abouzeid et al. recently demonstrated that alginate/PVA hydrogels can be prepared with bifunctional cellulose nanofibers with reactive carboxyl and aldehyde groups [139]. The 3D printed scaffold was able to demonstrate the ability to mineralize. However, there is still more work to be done to print a hydrogel construct that can withstand physiological load while maintaining precise control over fiber diameter and morphology due to the intrinsic effect of material properties on printing precision and overall scaffold mechanics.

4 Future Outlook and Conclusions

Nanotechnology has provided tissue engineers the ability to mimic native bone ECM and improve the bone regeneration process. Numerous nanomaterials have demonstrated immense potential in bone bioprinting applications since they present nanoscale cues that can positively impact osteogenic attachment and differentiation. Additionally, various nanocomposites have displayed improved mechanical and biological properties in bioprinted bone scaffolds. Many of the scaffolds incorporated with nanoparticles have displayed the capacity to better mimic the complex properties of the natural bone environment that can promote cellular attachment, ingrowth, and bone formation. However, there are still questions regarding the interactions between the nanosurface topography and the osteal defects into which these enhanced scaffolds are introduced. Furthermore, new design strategies and fabrication methods will need to be expanded upon experimentally to be ultimately tailored

for complex bone defect repair treatment in the clinic. Also, large animal model studies that confirm that these scaffolds support vascularization and bone formation in clinically sized defects are still needed. Tissue engineers will need to examine the nanomaterials within structures that best support bone regeneration in a controlled manner. Ultimately, future research will need to overcome current challenges of bone regeneration and expand the multifunctional capabilities of nanomaterials for BTE.

References

1. Li X, Wang L, Fan Y, Feng Q, Cui FZ, Watari F. Nanostructured scaffolds for bone tissue engineering. *J Biomed Mater Res A*. 2013;101(8):2424–35.
2. Lopes D, Martins-Cruz C, Oliveira MB, Mano JF. Bone physiology as inspiration for tissue regenerative therapies. *Biomaterials*. 2018;185:240–75.
3. Nair AK, Gautieri A, Chang SW, Buehler MJ. Molecular mechanics of mineralized collagen fibrils in bone. *Nat Commun*. 2013;4:1724.
4. Gerdes S, Mostafavi A, Ramesh S, Memic A, Rivero IV, Rao P, Tamayol A. Process-structure-quality relationships of three-dimensional printed poly(Caprolactone)-hydroxyapatite scaffolds. *Tissue Eng Part A*. 2020;26(5–6):279–91.
5. Griffin MF, Kalaskar DM, Seifalian A, Butler PE. An update on the application of nanotechnology in bone tissue engineering. *Open Orthop J*. 2016;10:836–48.
6. Sun L, Stout DA, Webster TJ. The nano-effect: improving the long-term prognosis for musculoskeletal implants. *J Long-Term Eff Med Implants*. 2012;22(3):195–209.
7. Gong T, Xie J, Liao J, Zhang T, Lin S, Lin Y. Nanomaterials and bone regeneration. *Bone Res*. 2015;3:15029.
8. Moreno Madrid AP, Vrech SM, Sanchez MA, Rodriguez AP. Advances in additive manufacturing for bone tissue engineering scaffolds. *Mater Sci Eng C Mater Biol Appl*. 2019;100:631–44.
9. Tang D, Tare RS, Yang LY, Williams DF, Ou KL, Oreffo RO. Biofabrication of bone tissue: approaches, challenges and translation for bone regeneration. *Biomaterials*. 2016;83:363–82.
10. Midha S, Dalela M, Sybil D, Patra P, Mohanty S. Advances in three-dimensional bioprinting of bone: progress and challenges. *J Tissue Eng Regen Med*. 2019;13(6):925–45.
11. Rider P, Kacarevic ZP, Alkildani S, Retnasingh S, Schnettler R, Barbeck M. Additive manufacturing for guided bone regeneration: a perspective for alveolar ridge augmentation. *Int J Mol Sci*. 2018;19(11):3308.
12. Nyberg E, Rindone A, Dorafshar A, Grayson WL. Comparison of 3D-printed poly- ϵ -caprolactone scaffolds functionalized with tricalcium phosphate, hydroxyapatite, Bio-Oss, or decellularized bone matrix. *Tissue Eng A*. 2016;23(11–12):503–14.
13. Ashammakhi N, Hasan A, Kaarela O, Byambaa B, Sheikhi A, Gaharwar AK, Khademhosseini A. Advancing frontiers in bone bioprinting. *Adv Healthc Mater*. 2019;8(7):e1801048.
14. Lee JY, Choi B, Wu B, Lee M. Customized biomimetic scaffolds created by indirect three-dimensional printing for tissue engineering. *Biofabrication*. 2013;5(4):045003.
15. Huang J, Gräter SV, Corbellini F, Rinck S, Bock E, Kemkemer R, Kessler H, Ding J, Spatz JP. Impact of order and disorder in RGD nanopatterns on cell adhesion. *Nano Lett*. 2009;9(3):1111–6.
16. Ahn EH, Kim Y, Kshitiz, An SS, Afzal J, Lee S, Kwak M, Suh KY, Kim DH, Levchenko A. Spatial control of adult stem cell fate using nanotopographic cues. *Biomaterials*. 2014;35(8):2401–10.

17. Guilak F, Cohen DM, Estes BT, Gimble JM, Liedtke W, Chen CS. Control of stem cell fate by physical interactions with the extracellular matrix. *Cell Stem Cell*. 2009;5(1):17–26.
18. Chen G, Lv Y. Immobilization and application of electrospun nanofiber scaffold-based growth factor in bone tissue engineering. *Curr Pharm Des*. 2015;21(15):1967–78.
19. Nyberg E, Holmes C, Witham T, Grayson WL. Growth factor-eluting technologies for bone tissue engineering. *Drug Deliv Transl Res*. 2016;6(2):184–94.
20. Walmsley GG, McArdle A, Tevlin R, Momeni A, Atashrood D, Hu MS, Feroze AH, Wong VW, Lorenz PH, Longaker MT, Wan DC. Nanotechnology in bone tissue engineering. *Nanomedicine*. 2015;11(5):1253–63.
21. Uskokovic V, Desai TA. Nanoparticulate drug delivery platforms for advancing bone infection therapies. *Expert Opin Drug Deliv*. 2014;11(12):1899–912.
22. Wang C, Zhao Q, Wang M. Cryogenic 3D printing for producing hierarchical porous and rhBMP-2-loaded Ca-P/PLLA nanocomposite scaffolds for bone tissue engineering. *Biofabrication*. 2017;9(2):025031.
23. Correia TR, Figueira DR, de Sa KD, Miguel SP, Fradique RG, Mendonca AG, Correia IJ. 3D printed scaffolds with bactericidal activity aimed for bone tissue regeneration. *Int J Biol Macromol*. 2016;93(Pt B):1432–45.
24. Tovar N, Witek L, Atria P, Sobieraj M, Bowers M, Lopez CD, Cronstein BN, Coelho PG. Form and functional repair of long bone using 3D-printed bioactive scaffolds. *J Tissue Eng Regen Med*. 2018;12(9):1986–99.
25. Wang C, Ye X, Zhao Y, Bai L, He Z, Tong Q, Xie X, Zhu H, Cai D, Zhou Y, Lu B, Wei Y, Mei L, Xie D, Wang M. Cryogenic 3D printing of porous scaffolds for in situ delivery of 2D black phosphorus nanosheets, doxorubicin hydrochloride and osteogenic peptide for treating tumor resection-induced bone defects. *Biofabrication*. 2020;12(3):035004.
26. Zhang Y, Zhai D, Xu M, Yao Q, Zhu H, Chang J, Wu C. 3D-printed bioceramic scaffolds with antibacterial and osteogenic activity. *Biofabrication*. 2017;9(2):025037.
27. Song Y, Lin K, He S, Wang C, Zhang S, Li D, Wang J, Cao T, Bi L, Pei G. Nano-biphasic calcium phosphate/polyvinyl alcohol composites with enhanced bioactivity for bone repair via low-temperature three-dimensional printing and loading with platelet-rich fibrin. *Int J Nanomedicine*. 2018;13:505–23.
28. Martin V, Ribeiro IA, Alves MM, Goncalves L, Claudio RA, Grenho L, Fernandes MH, Gomes P, Santos CF, Bettencourt AF. Engineering a multifunctional 3D-printed PLA-collagen-minocycline-nanoHydroxyapatite scaffold with combined antimicrobial and osteogenic effects for bone regeneration. *Mater Sci Eng C Mater Biol Appl*. 2019;101:15–26.
29. Chen S, Shi Y, Zhang X, Ma J. Biomimetic synthesis of Mg-substituted hydroxyapatite nanocomposites and three-dimensional printing of composite scaffolds for bone regeneration. *J Biomed Mater Res A*. 2019;107(11):2512–21.
30. Luo Y, Chen S, Shi Y, Ma J. 3D printing of strontium-doped hydroxyapatite based composite scaffolds for repairing critical-sized rabbit calvarial defects. *Biomed Mater*. 2018;13(6):065004.
31. Bas O, Hansske F, Lim J, Ravichandran A, Kemnitz E, Teoh SH, Hutmacher DW, Borner HG. Tuning mechanical reinforcement and bioactivity of 3D printed ternary nanocomposites by interfacial peptide-polymer conjugates. *Biofabrication*. 2019;11(3):035028.
32. Castro NJ, O'Brien J, Zhang LG. Integrating biologically inspired nanomaterials and table-top stereolithography for 3D printed biomimetic osteochondral scaffolds. *Nanoscale*. 2015;7(33):14010–22.
33. Chen S, Shi Y, Luo Y, Ma J. Layer-by-layer coated porous 3D printed hydroxyapatite composite scaffolds for controlled drug delivery. *Colloids Surf B Biointerfaces*. 2019;179:121–7.
34. Chen X, Gao C, Jiang J, Wu Y, Zhu P, Chen G. 3D printed porous PLA/nHA composite scaffolds with enhanced osteogenesis and osteoconductivity in vivo for bone regeneration. *Biomed Mater*. 2019;14(6):065003.
35. Demirtas TT, Irmak G, Gumusderelioglu M. A bioprintable form of chitosan hydrogel for bone tissue engineering. *Biofabrication*. 2017;9(3):035003.

36. Deng N, Sun J, Li Y, Chen L, Chen C, Wu Y, Wang Z, Li L. Experimental study of rhBMP-2 chitosan nano-sustained release carrier-loaded PLGA/nHA scaffolds to construct mandibular tissue-engineered bone. *Arch Oral Biol*. 2019;102:16–25.
37. Gao C, Deng Y, Feng P, Mao Z, Li P, Yang B, Deng J, Cao Y, Shuai C, Peng S. Current progress in bioactive ceramic scaffolds for bone repair and regeneration. *Int J Mol Sci*. 2014;15(3):4714–32.
38. Goncalves EM, Oliveira FJ, Silva RF, Neto MA, Fernandes MH, Amaral M, Vallet-Regi M, Vila M. Three-dimensional printed PCL-hydroxyapatite scaffolds filled with CNTs for bone cell growth stimulation. *J Biomed Mater Res B Appl Biomater*. 2016;104(6):1210–9.
39. Holmes B, Bulusu K, Plesniak M, Zhang LG. A synergistic approach to the design, fabrication and evaluation of 3D printed micro and nano featured scaffolds for vascularized bone tissue repair. *Nanotechnology*. 2016;27(6):064001.
40. Prasopthum A, Shakesheff KM, Yang J. Direct three-dimensional printing of polymeric scaffolds with nanofibrous topography. *Biofabrication*. 2018;10(2):025002.
41. Rogowska-Tylman J, Locs J, Salma I, Wozniak B, Pilmane M, Zalite V, Wojnarowicz J, Kedzierska-Sar A, Chudoba T, Szlczak K, Chlanda A, Swieszkowski W, Gedanken A, Lojkowski W. In vivo and in vitro study of a novel nanohydroxyapatite sonocoated scaffolds for enhanced bone regeneration. *Mater Sci Eng C Mater Biol Appl*. 2019;99:669–84.
42. Roh HS, Lee CM, Hwang YH, Kook MS, Yang SW, Lee D, Kim BH. Addition of MgO nanoparticles and plasma surface treatment of three-dimensional printed polycaprolactone/hydroxyapatite scaffolds for improving bone regeneration. *Mater Sci Eng C Mater Biol Appl*. 2017;74:525–35.
43. Trachtenberg JE, Placone JK, Smith BT, Fisher JP, Mikos AG. Extrusion-based 3D printing of poly(propylene fumarate) scaffolds with hydroxyapatite gradients. *J Biomater Sci Polym Ed*. 2017;28(6):532–54.
44. Wang Q, Xia Q, Wu Y, Zhang X, Wen F, Chen X, Zhang S, Heng BC, He Y, Ouyang HW. 3D-printed Atsstrin-incorporated alginate/hydroxyapatite scaffold promotes bone defect regeneration with TNF/TNFR signaling involvement. *Adv Healthc Mater*. 2015;4(11):1701–8.
45. Yang WF, Long L, Wang R, Chen D, Duan S, Xu FJ. Surface-modified hydroxyapatite nanoparticle-reinforced polylactides for three-dimensional printed bone tissue engineering scaffolds. *J Biomed Nanotechnol*. 2018;14(2):294–303.
46. Yu J, Xu Y, Li S, Seifert GV, Becker ML. Three-dimensional printing of nano hydroxyapatite/poly(ester urea) composite scaffolds with enhanced bioactivity. *Biomacromolecules*. 2017;18(12):4171–83.
47. Zhou X, Esworthy T, Lee SJ, Miao S, Cui H, Plesiniak M, Fenniri H, Webster T, Rao RD, Zhang LG. 3D printed scaffolds with hierarchical biomimetic structure for osteochondral regeneration. *Nanomedicine*. 2019;19:58–70.
48. Ciapetti G, Di Pompo G, Avnet S, Martini D, Diez-Escudero A, Montufar EB, Ginebra MP, Baldini N. Osteoclast differentiation from human blood precursors on biomimetic calcium-phosphate substrates. *Acta Biomater*. 2017;50:102–13.
49. Muller P, Bulnheim U, Diener A, Luthen F, Teller M, Klinkenberg ED, Neumann HG, Nebe B, Liebold A, Steinhoff G, Rychly J. Calcium phosphate surfaces promote osteogenic differentiation of mesenchymal stem cells. *J Cell Mol Med*. 2008;12(1):281–91.
50. Samavedi S, Whittington AR, Goldstein AS. Calcium phosphate ceramics in bone tissue engineering: a review of properties and their influence on cell behavior. *Acta Biomater*. 2013;9(9):8037–45.
51. Jeong J, Kim JH, Shim JH, Hwang NS, Heo CY. Bioactive calcium phosphate materials and applications in bone regeneration. *Biomater Res*. 2019;23:4.
52. Yoshikawa H, Myoui A. Bone tissue engineering with porous hydroxyapatite ceramics. *J Artif Organs*. 2005;8(3):131–6.
53. Ramselaar MMA, Driessens FCM, Kalk W, De Wijn JR, Van Mullem PJ. Biodegradation of four calcium phosphate ceramics; in vivo rates and tissue interactions. *J Mater Sci Mater Med*. 1991;2(2):63–70.

54. Ramesh N, Moratti SC, Dias GJ. Hydroxyapatite-polymer biocomposites for bone regeneration: a review of current trends. *J Biomed Mater Res B Appl Biomater*. 2018;106(5):2046–57.
55. Li Y, Liu C. Nanomaterial-based bone regeneration. *Nanoscale*. 2017;9(15):4862–74.
56. Hong Z, Zhang P, Liu A, Chen L, Chen X, Jing X. Composites of poly(lactide-co-glycolide) and the surface modified carbonated hydroxyapatite nanoparticles. *J Biomed Mater Res A*. 2007;81(3):515–22.
57. LeGeros RZ. Properties of osteoconductive biomaterials: calcium phosphates. *Clin Orthop Relat Res*. 2002;395:81–98.
58. Sethu SN, Namashivayam S, Devendran S, Nagarajan S, Tsai WB, Narashiman S, Ramachandran M, Ambigapathi M. Nanoceramics on osteoblast proliferation and differentiation in bone tissue engineering. *Int J Biol Macromol*. 2017;98:67–74.
59. Suchanek W, Yoshimura M. Processing and properties of hydroxyapatite-based biomaterials for use as hard tissue replacement implants. *J Mater Res*. 1998;13(1):94–117.
60. Prakasam M, Locs J, Salma-Ancane K, Loca D, Largeteau A, Berzina-Cimdina L. Fabrication, properties and applications of dense hydroxyapatite: a review. *J Funct Biomater*. 2015;6(4):1099–140.
61. Wijerathne HMCS, Yan D, Zeng B, Xie Y, Hu H, Wickramaratne MN, Han Y. Effect of nano-hydroxyapatite on protein adsorption and cell adhesion of poly(lactic acid)/nano-hydroxyapatite composite microspheres. *SN Appl Sci*. 2020;2(4):722.
62. Wang X, Li Y, Wei J, de Groot K. Development of biomimetic nano-hydroxyapatite/poly(hexamethylene adipamide) composites. *Biomaterials*. 2002;23(24):4787–91.
63. Aydin E, Planell JA, Hasirci V. Hydroxyapatite nanorod-reinforced biodegradable poly(L-lactic acid) composites for bone plate applications. *J Mater Sci Mater Med*. 2011;22(11):2413–27.
64. Horch HH, Sader R, Pautke C, Neff A, Deppe H, Kolk A. Synthetic, pure-phase beta-tricalcium phosphate ceramic granules (Cerasorb) for bone regeneration in the reconstructive surgery of the jaws. *Int J Oral Maxillofac Surg*. 2006;35(8):708–13.
65. Yamada S, Heymann D, Boulter JM, Daculsi G. Osteoclastic resorption of calcium phosphate ceramics with different hydroxyapatite/beta-tricalcium phosphate ratios. *Biomaterials*. 1997;18(15):1037–41.
66. Kamitakahara M, Ohtsuki C, Miyazaki T. Review paper: behavior of ceramic biomaterials derived from tricalcium phosphate in physiological condition. *J Biomater Appl*. 2008;23(3):197–212.
67. Dorozhkin SV. Biphasic, triphasic and multiphasic calcium orthophosphates. *Acta Biomater*. 2012;8(3):963–77.
68. Combes C, Rey C. Amorphous calcium phosphates: synthesis, properties and uses in biomaterials. *Acta Biomater*. 2010;6(9):3362–78.
69. Leite AJ, Mano JF. Biomedical applications of natural-based polymers combined with bioactive glass nanoparticles. *J Mater Chem B*. 2017;5(24):4555–68.
70. Saravanapavan P, Jones JR, Pryce RS, Hench LL. Bioactivity of gel-glass powders in the CaO-SiO₂ system: a comparison with ternary (CaO-P₂O₅-SiO₂) and quaternary glasses (SiO₂-CaO-P₂O₅-Na₂O). *J Biomed Mater Res A*. 2003;66(1):110–9.
71. Saravanapavan P, Jones JR, Verrier S, Beilby R, Shirliff VJ, Hench LL, Polak JM. Binary CaO-SiO₂ gel-glasses for biomedical applications. *Biomed Mater Eng*. 2004;14(4):467–86.
72. Wang X, Li W. Biodegradable mesoporous bioactive glass nanospheres for drug delivery and bone tissue regeneration. *Nanotechnology*. 2016;27(22):225102.
73. Liang Q, Hu Q, Miao G, Yuan B, Chen X. A facile synthesis of novel mesoporous bioactive glass nanoparticles with various morphologies and tunable mesostructure by sacrificial liquid template method. *Mater Lett*. 2015;148:45–9.
74. Li Y, Chen X, Ning C, Yuan B, Hu Q. Facile synthesis of mesoporous bioactive glasses with controlled shapes. *Mater Lett*. 2015;161:605–8.
75. Geng Y, Dalhaimer P, Cai S, Tsai R, Tewari M, Minko T, Discher DE. Shape effects of filaments versus spherical particles in flow and drug delivery. *Nat Nanotechnol*. 2007;2(4):249–55.

76. Cui F-Z, Li Y, Ge J. Self-assembly of mineralized collagen composites. *Mater Sci Eng R Rep.* 2007;57(1):1–27.
77. Rocton N, Oudadesse H, Mosbahi S, Bunetel L, Pellen-Mussi P, Lefeuvre B. Study of nano bioactive glass for use as bone biomaterial comparison with micro bioactive glass behaviour. *IOP Conf Ser Mater Sci Eng.* 2019;628:012005.
78. Ajita J, Saravanan S, Selvamurugan N. Effect of size of bioactive glass nanoparticles on mesenchymal stem cell proliferation for dental and orthopedic applications. *Mater Sci Eng C Mater Biol Appl.* 2015;53:142–9.
79. Chen YW, Shen YF, Ho CC, Yu J, Wu YA, Wang K, Shih CT, Shie MY. Osteogenic and angiogenic potentials of the cell-laden hydrogel/mussel-inspired calcium silicate complex hierarchical porous scaffold fabricated by 3D bioprinting. *Mater Sci Eng C Mater Biol Appl.* 2018;91:679–87.
80. Chen M, Zhao F, Li Y, Wang M, Chen X, Lei B. 3D-printed photoluminescent bioactive scaffolds with biomimetic elastomeric surface for enhanced bone tissue engineering. *Mater Sci Eng C Mater Biol Appl.* 2020;106:110153.
81. Dang W, Li T, Li B, Ma H, Zhai D, Wang X, Chang J, Xiao Y, Wang J, Wu C. A bifunctional scaffold with CuFeSe₂ nanocrystals for tumor therapy and bone reconstruction. *Biomaterials.* 2018;160:92–106.
82. Gao G, Schilling AF, Yonezawa T, Wang J, Dai G, Cui X. Bioactive nanoparticles stimulate bone tissue formation in bioprinted three-dimensional scaffold and human mesenchymal stem cells. *Biotechnol J.* 2014;9(10):1304–11.
83. Ojansivu M, Rashad A, Ahlinder A, Massera J, Mishra A, Syverud K, Finne-Wistrand A, Miettinen S, Mustafa K. Wood-based nanocellulose and bioactive glass modified gelatin-alginate bioinks for 3D bioprinting of bone cells. *Biofabrication.* 2019;11(3):035010.
84. Zhu M, Li K, Zhu Y, Zhang J, Ye X. 3D-printed hierarchical scaffold for localized isoniazid/rifampin drug delivery and osteoarticular tuberculosis therapy. *Acta Biomater.* 2015;16:145–55.
85. Carrow JK, Di Luca A, Dolatshahi-Pirouz A, Moroni L, Gaharwar AK. 3D-printed bioactive scaffolds from nanosilicates and PEOT/PBT for bone tissue engineering. *Regen Biomater.* 2019;6(1):29–37.
86. Cidonio G, Alcalá-Orozco CR, Lim KS, Glinka M, Mutreja I, Kim YH, Dawson JI, Woodfield TB, Oreffo ROC. Osteogenic and angiogenic tissue formation in high fidelity nanocomposite Laponite-gelatin bioinks. *Biofabrication.* 2019;11(3):035027.
87. Cidonio G, Cooke M, Glinka M, Dawson JI, Grover L, Oreffo ROC. Printing bone in a gel: using nanocomposite bioink to print functionalised bone scaffolds. *Mater Today Bio.* 2019;4:100028.
88. Cidonio G, Glinka M, Kim YH, Kanczler JM, Lanham SA, Ahlfeld T, Lode A, Dawson JI, Gelinsky M, Oreffo ROC. Nanoclay-based 3D printed scaffolds promote vascular ingrowth ex vivo and generate bone mineral tissue in vitro and in vivo. *Biofabrication.* 2020;12(3):035010.
89. Zhai X, Ruan C, Ma Y, Cheng D, Wu M, Liu W, Zhao X, Pan H, Lu WW. 3D-bioprinted osteoblast-laden nanocomposite hydrogel constructs with induced microenvironments promote cell viability, differentiation, and osteogenesis both in vitro and in vivo. *Adv Sci (Weinh).* 2018;5(3):1700550.
90. Luo Z, Zhang S, Pan J, Shi R, Liu H, Lyu Y, Han X, Li Y, Yang Y, Xu Z, Sui Y, Luo E, Zhang Y, Wei S. Time-responsive osteogenic niche of stem cells: a sequentially triggered, dual-peptide loaded, alginate hybrid system for promoting cell activity and osteo-differentiation. *Biomaterials.* 2018;163:25–42.
91. Zhang Y, Yu W, Ba Z, Cui S, Wei J, Li H. 3D-printed scaffolds of mesoporous bioglass/gliadin/polycaprolactone ternary composite for enhancement of compressive strength, degradability, cell responses and new bone tissue ingrowth. *Int J Nanomedicine.* 2018;13:5433–47.

92. Ottria L, Lauritano D, Andreasi Bassi M, Palmieri A, Candotto V, Tagliabue A, Tettamanti L. Mechanical, chemical and biological aspects of titanium and titanium alloys in implant dentistry. *J Biol Regul Homeost Agents*. 2018;32(2 Suppl. 1):81–90.
93. Yang J, Chen HJ, Zhu XD, Vaidya S, Xiang Z, Fan YJ, Zhang XD. Enhanced repair of a critical-sized segmental bone defect in rabbit femur by surface microstructured porous titanium. *J Mater Sci Mater Med*. 2014;25(7):1747–56.
94. Rasoulianboroujeni M, Fahimpour F, Shah P, Khoshroo K, Tahriri M, Eslami H, Yadegari A, Dashtimoghadam E, Tayebi L. Development of 3D-printed PLGA/TiO₂ nanocomposite scaffolds for bone tissue engineering applications. *Mater Sci Eng C Mater Biol Appl*. 2019;96:105–13.
95. Marino A, Barsotti J, de Vito G, Filippeschi C, Mazzolai B, Piazza V, Labardi M, Mattoli V, Ciofani G. Two-photon lithography of 3D nanocomposite piezoelectric scaffolds for cell stimulation. *ACS Appl Mater Interfaces*. 2015;7(46):25574–9.
96. Nabyouni M, Bruckner T, Zhou H, Gbureck U, Bhaduri SB. Magnesium-based bioceramics in orthopedic applications. *Acta Biomater*. 2018;66:23–43.
97. Seebach E, Kubatzky KF. Chronic implant-related bone infections-can immune modulation be a therapeutic strategy? *Front Immunol*. 2019;10:1724.
98. Jia Z, Xiu P, Xiong P, Zhou W, Cheng Y, Wei S, Zheng Y, Xi T, Cai H, Liu Z, Wang C, Zhang W, Li Z. Additively manufactured macroporous titanium with silver-releasing micro-/nanoporous surface for multipurpose infection control and bone repair - a proof of concept. *ACS Appl Mater Interfaces*. 2016;8(42):28495–510.
99. Deng L, Deng Y, Xie K. AgNPs-decorated 3D printed PEEK implant for infection control and bone repair. *Colloids Surf B Biointerfaces*. 2017;160:483–92.
100. Zou F, Jiang J, Lv F, Xia X, Ma X. Preparation of antibacterial and osteoconductive 3D-printed PLGA/Cu(I)@ZIF-8 nanocomposite scaffolds for infected bone repair. *J Nanobiotechnol*. 2020;18(1):39.
101. Zhu Y, Liu K, Deng J, Ye J, Ai F, Ouyang H, Wu T, Jia J, Cheng X, Wang X. 3D printed zirconia ceramic hip joint with precise structure and broad-spectrum antibacterial properties. *Int J Nanomedicine*. 2019;14:5977–87.
102. Dadfar SM, Roemhild K, Drude NI, von Stillfried S, Knuchel R, Kiessling F, Lammers T. Iron oxide nanoparticles: diagnostic, therapeutic and theranostic applications. *Adv Drug Deliv Rev*. 2019;138:302–25.
103. Shimizu K, Ito A, Yoshida T, Yamada Y, Ueda M, Honda H. Bone tissue engineering with human mesenchymal stem cell sheets constructed using magnetite nanoparticles and magnetic force. *J Biomed Mater Res B Appl Biomater*. 2007;82(2):471–80.
104. Huang J, Liu W, Liang Y, Li L, Duan L, Chen J, Zhu F, Lai Y, Zhu W, You W, Jia Z, Xiong J, Wang D. Preparation and biocompatibility of diphasic magnetic nanocomposite scaffold. *Mater Sci Eng C Mater Biol Appl*. 2018;87:70–7.
105. Jackson RJ, Patrick PS, Page K, Powell MJ, Lythgoe MF, Miodownik MA, Parkin IP, Carmalt CJ, Kalber TL, Bear JC. Chemically treated 3D printed polymer scaffolds for biomineral formation. *ACS Omega*. 2018;3(4):4342–51.
106. Chang WJ, Pan YH, Tzeng JJ, Wu TL, Fong TH, Feng SW, Huang HM. Development and testing of X-ray imaging-enhanced poly-L-Lactide bone screws. *PLoS One*. 2015;10(10):e0140354.
107. Vial S, Reis RL, Oliveira J. Recent advances using gold nanoparticles as a promising multimodal tool for tissue engineering and regenerative medicine. *Curr Opin Solid State Mater Sci*. 2017;21(2):92–112.
108. Ko WK, Heo DN, Moon HJ, Lee SJ, Bae MS, Lee JB, Sun IC, Jeon HB, Park HK, Kwon IK. The effect of gold nanoparticle size on osteogenic differentiation of adipose-derived stem cells. *J Colloid Interface Sci*. 2015;438:68–76.
109. Li JJ, Kawazoe N, Chen G. Gold nanoparticles with different charge and moiety induce differential cell response on mesenchymal stem cell osteogenesis. *Biomaterials*. 2015;54:226–36.

110. Schwab EH, Pohl TL, Haraszti T, Schwaerzer GK, Hiepen C, Spatz JP, Knaus P, Cavalcanti-Adam EA. Nanoscale control of surface immobilized BMP-2: toward a quantitative assessment of BMP-mediated signaling events. *Nano Lett.* 2015;15(3):1526–34.
111. Ryoo SR, Kim YK, Kim MH, Min DH. Behaviors of NIH-3T3 fibroblasts on graphene/carbon nanotubes: proliferation, focal adhesion, and gene transfection studies. *ACS Nano.* 2010;4(11):6587–98.
112. Choe G, Oh S, Seok JM, Park SA, Lee JY. Graphene oxide/alginate composites as novel bioinks for three-dimensional mesenchymal stem cell printing and bone regeneration applications. *Nanoscale.* 2019;11(48):23275–85.
113. Belaid H, Nagarajan S, Teyssier C, Barou C, Bares J, Balme S, Garay H, Huon V, Cornu D, Cavailles V, Bechelany M. Development of new biocompatible 3D printed graphene oxide-based scaffolds. *Mater Sci Eng C Mater Biol Appl.* 2020;110:110595.
114. Pei B, Wang W, Dunne N, Li X. Applications of carbon nanotubes in bone tissue regeneration and engineering: superiority, concerns, current advancements, and prospects. *Nanomaterials (Basel).* 2019;9(10):1501.
115. Shao W, Paul A, Zhao B, Lee C, Rodes L, Prakash S. Carbon nanotube lipid drug approach for targeted delivery of a chemotherapy drug in a human breast cancer xenograft animal model. *Biomaterials.* 2013;34(38):10109–19.
116. Munir K, Wen C, Li Y. Carbon nanotubes and graphene as nanoreinforcements in metallic biomaterials: a review. *Adv Biosyst.* 2019;3:e1800212.
117. Gerasimenko A, Ichkitidze L, Podgaetskii V, Selishchev S. Biomedical applications of promising nanomaterials with carbon nanotubes. *Biomed Eng.* 2015;48:310–4.
118. Khalid P, Suman V. Carbon nanotube-hydroxyapatite composite for bone tissue engineering and their interaction with mouse fibroblast L929 in vitro. *J Bionanosci.* 2017;11:233–40.
119. Tutak W, Chowalla M, Sesti F. The chemical and physical characteristics of single-walled carbon nanotube film impact on osteoblastic cell response. *Nanotechnology.* 2010;21(31):315102.
120. Zhang F, Weidmann A, Nebe JB, Burkel E. Osteoblast cell response to surface-modified carbon nanotubes. *Mater Sci Eng C.* 2012;32(5):1057–61.
121. Huang B, Vyas C, Roberts I, Poutrel QA, Chiang WH, Blaker JJ, Huang Z, Bartolo P. Fabrication and characterisation of 3D printed MWCNT composite porous scaffolds for bone regeneration. *Mater Sci Eng C Mater Biol Appl.* 2019;98:266–78.
122. Liu X, George MN, Park S, Miller Ii AL, Gaihre B, Li L, Waletzki BE, Terzc A, Yaszemski MJ, Lu L. 3D-printed scaffolds with carbon nanotubes for bone tissue engineering: fast and homogeneous one-step functionalization. *Acta Biomater.* 2020;111:129.
123. Cui H, Yu Y, Li X, Sun Z, Ruan J, Wu Z, Qian J, Yin J. Direct 3D printing of a tough hydrogel incorporated with carbon nanotubes for bone regeneration. *J Mater Chem B.* 2019;7(45):7207–17.
124. Donnalaja F, Jacchetti E, Soncini M, Raimondi MT. Natural and synthetic polymers for bone scaffolds optimization. *Polymers.* 2020;12(4):905.
125. Sonaje K, Italia JL, Sharma G, Bhardwaj V, Tikoo K, Kumar MNVR. Development of biodegradable nanoparticles for Oral delivery of Ellagic acid and evaluation of their antioxidant efficacy against cyclosporine A-induced nephrotoxicity in rats. *Pharm Res.* 2007;24(5):899–908.
126. Jain A, Jain A, Gulbake A, Shilpi S, Hurkat P, Jain SK. Peptide and protein delivery using new drug delivery systems. *Crit Rev Ther Drug Carrier Syst.* 2013;30(4):293–329.
127. Rai R, Alwani S, Badea I. Polymeric nanoparticles in gene therapy: new avenues of design and optimization for delivery applications. *Polymers.* 2019;11(4):745.
128. Hassan AH, Hosny KM, Murshid ZA, Alhadlaq A, Alyamani A, Naguib G. Depot injectable biodegradable nanoparticles loaded with recombinant human bone morphogenetic protein-2: preparation, characterization, and in vivo evaluation. *Drug Des Devel Ther.* 2015;9:3599–606.
129. Kim BS, Yang SS, Kim CS. Incorporation of BMP-2 nanoparticles on the surface of a 3D-printed hydroxyapatite scaffold using an epsilon-polycaprolactone polymer emulsion coating method for bone tissue engineering. *Colloids Surf B Biointerfaces.* 2018;170:421–9.

130. Liu S, He Z, Xu G, Xiao X. Fabrication of polycaprolactone nanofibrous scaffolds by facile phase separation approach. *Mater Sci Eng C Mater Biol Appl*. 2014;44:201–8.
131. Xu H, Cao B, George A, Mao C. Self-assembly and mineralization of genetically modifiable biological nanofibers driven by beta-structure formation. *Biomacromolecules*. 2011;12(6):2193–9.
132. Guo Z, Xu J, Ding S, Li H, Zhou C, Li L. In vitro evaluation of random and aligned polycaprolactone/gelatin fibers via electrospinning for bone tissue engineering. *J Biomater Sci Polym Ed*. 2015;26(15):989–1001.
133. Yao Q, Cosme JG, Xu T, Miszuk JM, Picciani PH, Fong H, Sun H. Three dimensional electrospun PCL/PLA blend nanofibrous scaffolds with significantly improved stem cells osteogenic differentiation and cranial bone formation. *Biomaterials*. 2017;115:115–27.
134. Sisson K, Zhang C, Farach-Carson MC, Chase DB, Rabolt JF. Fiber diameters control osteoblastic cell migration and differentiation in electrospun gelatin. *J Biomed Mater Res A*. 2010;94(4):1312–20.
135. Li R, McCarthy A, Zhang YS, Xie J. Decorating 3D printed scaffolds with electrospun nanofiber segments for tissue engineering. *Adv Biosyst*. 2019;3(12):1900137.
136. Mendoza-Buenrostro C, Lara H, Rodriguez C. Hybrid fabrication of a 3D printed geometry embedded with PCL nanofibers for tissue engineering applications. *Proc Eng*. 2015;110:128–34.
137. Vazquez-Vazquez FC, Chanes-Cuevas OA, Masuoka D, Alatorre JA, Chavarria-Bolaños D, Vega-Baudrit JR, Serrano-Bello J, Alvarez-Perez MA. Biocompatibility of developing 3D-printed tubular scaffold coated with nanofibers for bone applications. *J Nanomater*. 2019;2019:6105818.
138. Placone JK, Mahadik B, Fisher JP. Addressing present pitfalls in 3D printing for tissue engineering to enhance future potential. *APL Bioeng*. 2020;4(1):010901.
139. Abouzeid RE, Khiari R, Salama A, Diab M, Beneventi D, Dufresne A. In situ mineralization of nano-hydroxyapatite on bifunctional cellulose nanofiber/polyvinyl alcohol/sodium alginate hydrogel using 3D printing. *Int J Biol Macromol*. 2020;160:538–47.